Homogeneous and Heterogeneous Electron Transfer Dynamics of Osmium-Containing Monolayers at the Air/Water Interface

Robert J. Forster*

National Center for Sensor Research, School of Chemical Sciences, Dublin City University, Dublin 9, Ireland

Tia E. Keyes

School of Chemistry, Dublin Institute of Technology, Kevin St., Dublin 8, Ireland

Marcin Majda

Department of Chemistry, University of California at Berkeley, Berkeley, California 94720-1460

Received: September 14, 1999; In Final Form: February 14, 2000

Langmuir monolayers have been formed at the air/water interface using $[Os(dpp)_2Qbpy](ClO_4)_2$, where dpp is 4,7-diphenyl-1,10-phenanthroline and Qbpy is 2,2′:4,4″:4′4″-quarterpyridyl. The mean molecular area decreases in a sigmoidal manner from 128 ± 1.25 to 119 ± 1.6 Å^2 as the pH of the subphase is increased from 3.0 to 7.0. Over the range $3.0 \leq pH \leq 7.0$ a single pK_a of 4.3 ± 0.3 is observed for the unbound Qbpy pyridine nitrogens when confined within a Langmuir monolayer. In solution, over the range $1.6 \leq pH \leq 7.0$ two pK_as of 3.2 ± 0.2 and 4.3 ± 0.2 are observed. Horizontal touch voltammetry, performed using microelectrodes, has been used to determine the apparent charge transport diffusion coefficients, D_{app}, as the mean molecular area is systematically varied. For surface concentrations, Γ, between approximately 1.0×10^{-10} and 1.4×10^{-10} mol cm^{-2}, the monolayer is in a liquid state and D_{app} increases linearly with increasing surface concentration. Although surface concentration dependent physical diffusion of the complexes prevents an accurate determination of the self-exchange rate constant, k_{ex}, analyzing these data in accordance with a 2-D Dahms−Ruff approach provides a lower bound of 1.0×10^8 M^{-1} s^{-1} for k_{ex}. When the monolayers are further compressed so that the molecular area is less than approximately 100 Å^2, charge transport proceeds via a percolation mechanism and the maximum value of the apparent diffusion coefficient, $D_{app,max}$, yields a rate constant for electron self-exchange between Os^{2+} and $Os^{3+}$of 1.6×10^9 M^{-1} s^{-1}. $D_{app,max}$ depends on the solution pH in a sigmoidal manner, increasing from approximately $6.6 \pm 0.2 \times 10^{-6}$ to $8.9 \pm 0.4 \times 10^{-6}$ cm^2 s^{-1} as the subphase pH is increased from 3.0 to 7.0. To probe the effect of molecular orientation on interfacial electron transfer rates, we have used chronoamperometry conducted on a microsecond time scale to measure the heterogeneous electron transfer rate, k, for both Langmuir and spontaneously adsorbed monolayers. In this way, the effect of making electrical contact through the Qbpy or dpp ligands on k can be probed. Although both rates are large, the rate measured at an overpotential of 50 mV for Langmuir monolayers ($1.7 \pm 0.2 \times 10^5$ s^{-1}) is approximately an order of magnitude smaller than that found for spontaneously absorbed systems ($1.2 \pm 0.3 \times 10^6$ s^{-1}), suggesting that the local microenvironment, e.g., packing density and molecular orientation, influence the rate of heterogeneous electron transfer in these systems.

Introduction

The formation, characterization, and electrochemical properties of structurally well-defined arrays of redox active molecules is important for a wide range of areas, including a fundamental understanding of electron transfer,[1] chemical sensing,[2] solar energy conversion,[3] and chromatography.[4] An important approach to realizing this objective is to use the Langmuir trough to form ordered films at the air/water interface. Moreover, by using a "line" electrode[5] the distance dependence of the 2-D lateral electron-transfer rate can be measured. For example, Majda and co-workers[6−8] have investigated the properties of osmium tris-4,7-diphenyl-1,10-phenanthroline perchlorate (dpp) monolayers at the air/water interface. Irrespective of the subphase pH, this compound forms solid 2-D aggregates on the water surface presumably because the molecule lacks an axis of polarity. Since these monolayers never exist in a liquid state, i.e., even when spread at high mean molecular area (MMA) both solid and gas phases coexist, $[Os(dpp)_3](ClO_4)_2$ films cannot be reversibly compressed and expanded.[7] The effect of the 2-D structure and morphology,[7,8] as well as solvent,[6] on the rate of lateral electron hopping has been investigated.

In this contribution, we report on Langmuir monolayers formed using $[Os(dpp)_2Qbpy](ClO_4)_2$ as a building block, where dpp is 4,7-diphenyl-1,10-phenanthroline and Qbpy is 2,2′:4,4″:4′4″-quarterpyridyl. Self-assembled monolayers of this type are known to show unusually ideal, reversible electrochemical responses over a wide range of surface concentrations.[9−14] This ideality, coupled with the ability of the Qbpy ligand to undergo protonation/deprotonation reactions, makes the monolayers attractive model systems for probing the distance dependence of two-dimensional electron transfer when used to form Langmuir layers at the air/water interface. An important objective is to understand how the rate of charge transport through this monolayer array is affected by changing the assembly's state

10.1021/jp9932620 CCC: $19.00 © 2000 American Chemical Society
Published on Web 04/12/2000

of charge. Indeed, one might expect that protonating the unbound pyridine nitrogens of the Qbpy would lead to the formation of liquid Langmuir monolayers that exhibit entirely different dynamics of lateral electron transport compared to solid films. Our lateral electron transport measurements reported below show that two different modes of charge propagation exist in these films depending on the pH and the extent of monolayer compression. In experiments where the subphase is acidic, the monolayer exists in a liquid state for low degrees of compression. Under these conditions,[15] electron transfer requires diffusional collision of the redox centers to form the precursor complex followed by electron transfer and diffusional separation of the centers back to their initial equilibrium positions. Thus, lateral electron transport in these expanded films requires both physical diffusion and electron self-exchange, and the corresponding rate constant can be estimated by probing the dependence of the apparent charge transport diffusion coefficient on the degree of monolayer compression. In contrast, at higher degrees of monolayer compression physical diffusion no longer contributes to the charge transport mechanism and 2-D percolation is a more appropriate model. In that region of surface concentrations, the apparent rate of electron hopping increase rapidly and reaches a maximum immediately prior to monolayer collapse. In the experiments reported here, we find that the rate of electron self-exchange within the solid films is an order of magnitude greater than that obtained in the liquid region. We postulate that for highly compressed monolayers, electron transfer occurs over a shorter Os−Os distance because the diphenylphenanthroline ligands interpenetrate. A decrease of reorganization energy due to weaker hydration of the compressed monolayer may also contribute to the fast electron hopping kinetics observed.

To probe the dynamics of the lateral charge transport, we have extended the capabilities of the horizontal touch voltammetry (HTV) technique pioneered by Fujuhira and Araki[16] and further developed by Bard and co-workers.[19,17] In this approach, a disk electrode is brought in contact with the monolayer at the air/water interface. Traditionally, voltammetry is performed at relatively fast scan rates to probe the dynamics of electroreduction and -oxidation of the redox centers trapped directly at the metal/subphase interface under the electrode. Here, we demonstrate that the slow scan voltammetric current observed at microelectrodes features an additional, diffusive component due to lateral charge propagation beyond the outer edge of the disk electrode. Thus, under these conditions, HTV allows us to probe the dynamics of lateral charge transport.

Beyond the issue of two-dimensional electron hopping, we have used chronoamperometry, conducted on a microsecond time scale,[9,12,18] to measure the rate of heterogeneous electron transfer across the electrode/monolayer interface for these Langmuir monolayers. In these on-trough HTV experiments, electrical contact is made through the "backside" of the monolayer, i.e., through the dpp ligands. This situation contrasts with spontaneously adsorbed monolayers of the same material in which Qbpy acts as the bridging ligand between the osmium metal center and the electrode surface.[12] By comparing heterogeneous electron-transfer rates for these two situations it ought to be possible to obtain an insight into the effect of the electron tunneling medium and the molecular orientation on heterogeneous electron-transfer processes.

Experimental Section

$[Os(dpp)_2(Qbpy)](ClO_4)_2$. 2,2′:4,4″:4′4″-Quarterpyridyl (0.15 g, 0.48 mM) was dissolved in ethanol/water (20 cm^3 60/40 v/v) and heated to reflux. *cis*-$Os(dpp)_2Cl_2$ (0.412 g, 0.45 mM) was dissolved in ethanol and added to the refluxing solution over 20 min. The reaction mixture was allowed to reflux for a further 16 h. The solvent volume was then reduced to 10 mL, and a solution of concentrated aqueous $NaClO_4$ was added. The resulting solid (0.493 g, 80% yield) was collected by filtration and recrystallized from acetone/water (1/1 v/v). The purity of the complex was confirmed by C, H, N analysis (calcd for $OsC_{68}H_{46}N_8Cl_2O_8$: C, 59.86; H, 3.37; N, 8.21. Found: C, 58.60; H, 3.22, N, 8.03), HPLC, and NMR.

Solution Phase pK_a. The pK_a of the $[Os(dpp)_2(Qbpy)]^{2+}$ complex was determined from UV−vis spectra recorded using a Shimadzu UV-2101PC spectrophotometer. Titrations in the pH range 1−8 were conducted in a potassium chloride/hydrochloric acid medium, containing 0.2 M KCl (25 cm^3) and 0.02 M HCl (48.5 cm^3). The pH was controlled by adding aliquots of concentrated HCl and NaOH. Spectroscopic changes were confirmed to be reversible by first decreasing and then increasing the solution pH between 1 and 8. No further spectroscopic changes were observed at pH values higher than 8. The pK_as were determined by fitting the spectroscopic changes occurring at 370 nm to the Henderson−Hasselbalch equation using nonlinear optimization procedures. The error on the pK_a values is approximately ±0.2.

Surface Pressure−Molecular Area (π−A) Isotherm. A circular, alternate layer Langmuir−Blodgett trough (Nima Technology, Model 2022) was used to record the surface pressure vs molecular area (π−A) isotherms and to carry out horizontal touch voltammetry. The surface pressures were measured to within ±0.1 mN/m using a Wilhelmy plate pressure sensor that was calibrated prior to use. The π−A isotherm of stearic acid was used to confirm the cleanliness of both the subphase and trough. Monolayers were spread from dilute chloroform solutions at an initial area per molecule of at least 500 $Å^2$ $molec^{-1}$. Each drop of solution was allowed to spread and the solvent evaporate prior to adding further material. A constant barrier speed of 50 cm^2 min^{-1}, corresponding to a compression rate of approximately 0.5 $Å^2$ $molec^{-1}$ s^{-1}, was used for recording π−A isotherms.

Horizontal Touch Voltammetry. Horizontal touch voltammograms were recorded as described by Bard and co-workers[19] using platinum microwires of radii between 1 and 12.5 μm sealed in a glass shroud that were mechanically polished and electrochemically cleaned as described previously.[18] After polishing, the soft glass tube creates a concentric glass shroud approximately 1.5 mm thick around the microdisk. All potentials are quoted with respect to a BAS Ag/AgCl gel-filled reference electrode. The potential of the ferrocene/ferricenium couple dissolved in acetonitrile containing 0.1 M TEAP as supporting electrolyte was +0.322 V. The large area platinum flag that acted as the auxiliary electrode and the reference were located behind the fixed barrier of the Langmuir trough. Cyclic voltammetry was performed using a CH Instruments model 660 electrochemical workstation. All subphases were thoroughly degassed using nitrogen, and a blanket of nitrogen was maintained over the trough during all experiments. Prior to measuring the voltammetric response, the monolayer was compressed to the desired surface pressure and allowed to stand for 10 min. The microelectrode was then moved down at a rate of 2 mm min^{-1} until it made contact with the monolayer surface before it was lifted upward by 0.5 mm at the same speed. This procedure avoids the possibility of vertically compressing the monolayer and/or disordering the assembly. The voltammetric response was recorded before and after the lifting operation to

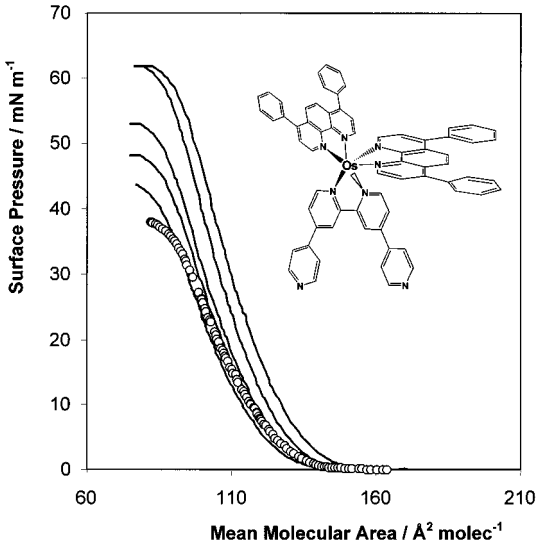

Figure 1. Structural formula for $[Os(dpp)_2Qbpy]^{2+}$. Open circles denote the $\pi-A$ isotherm for $[Os(dpp)_3]^{2+}$ on a subphase of 0.1 M $NaClO_4$. From top to bottom, the solid lines denote $\pi-A$ isotherms for the $[Os(dpp)_2Qbpy]^{2+}$ system at subphase pH values of 3.1, 4.0, 4.9, 6.1, and 7.0.

confirm that electrical contact had been established and that the procedure did not perturb the electrochemical properties of the film. The voltammetric response of the microelectrode was also investigated after it was forced through the monolayer into the subphase by a large amplitude vertical displacement at a rate of 2 mm min^{-1}.

Results and Discussion

***π*−*A* Isotherms.** Figure 1 illustrates the $\pi-A$ isotherms for $[Os(dpp)_2Qbpy](ClO_4)_2$ as the pH of the subphase is varied between 7.0 and 3.1 as well as for $[Os(dpp)_3](ClO_4)_2$, where the subphase is 0.1 M $NaClO_4$. For the $Os(dpp)_3$ system, the limiting area per molecule obtained by extrapolating the rising portion of the $\pi-A$ isotherm to zero surface pressure is 122 ± 5 $Å^2$, which agrees satisfactorily with the value of 127 ± 5 $Å^2$ previously reported by Majda and co-workers.[7,8] Where the subphase is 0.1 M $NaClO_4$, the limiting area observed for the Qbpy complex (119 ± 1.6 $Å^2$) is only marginally smaller than that observed for the $Os(dpp)_3$ complex (122 ± 5 $Å^2$). That both limiting areas are significantly less than the area of approximately 230 $Å^2$ predicted by the geometric radius of the molecule suggests that the dpp ligands of both complexes interpenetrate when the monolayers are highly compressed. However, the isotherms of the two compounds exhibit very different behavior when the barrier is reversed. As first described by Charych and co-workers,[7] $Os(dpp)_3$ monolayers exist as solid aggregates on the water surface. Consequently, the surface pressure rapidly drops to zero when the barrier is reversed. In contrast, for $3 \leq pH \leq 5$ the isotherms observed for monolayers of $[Os(dpp)_2Qbpy](ClO_4)_2$ can be reproduced over many cycles by compressing and subsequently allowing the monolayers to expand. This result suggests that the Qbpy complexes do not aggregate into solid 2-D islands but remain mobile on the water surface. Thus, the monolayers are 2-D liquids over nearly the entire range of measurable surface pressures. Monolayer collapse is observed when the system is compressed to molecular areas below ca. 80 $Å^2$ $molec^{-1}$.

When seeking to construct ordered assemblies for specific functions, e.g., in chemical sensing, display devices, vectorial electron transfer, and solar energy conversion, using individual molecules as building blocks, it is important to investigate how the molecule's properties change when it is incorporated within a supramolecular assembly. Toward this objective, we have investigated how the pK_as of the pyridine moieties of the quarterpyridyl ligand that are not bound to the osmium center change on going from solution to monolayer phases. Figure 2 shows the changes that occur in the visible region of the spectrum of the complex in solution as the pH is varied from 1.6 to 6.9. That the intensity and position of the metal-to-ligand-charge-transfer bands between approximately 410 and 850 nm remain largely unaffected by changes in the pH of the solution suggest that there is poor electronic communication between the Qbpy ligand and the metal center. However, the ligand-based $\pi-\pi^*$ transitions are sensitive to the solution pH allowing the pK_as to be determined. The change in absorbance at 370 nm is illustrated in the inset of Figure 2 and shows the sigmoidal shaped curve typically associated with acid−base equilibria. This curve is best described by the Henderson−Hasselbalch equation for a reaction involving two distinct protonation sites, and nonlinear optimization procedures provide best fit estimates of the pK_as as 3.2 and 4.3.

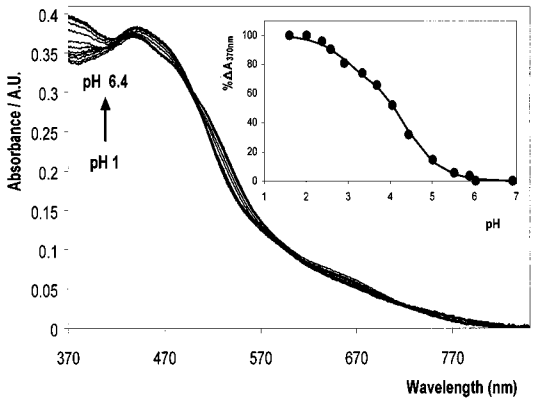

Figure 2. Changes in the UV−visible spectrum of $[Os(dpp)_2Qbpy](ClO_4)_2$ in water/acetonitrile (95:5 v/v) as the pH is systematically varied from 1.6 to 6.9. The inset shows the change in absorbance observed at 370 nm and the best fit obtained to the Henderson−Haselbalch equation using pK_a values of 4.3 and 3.2.

To probe the pK_a of the Qbpy moieties within the monolayer, we have investigated the dependence of both the collapse pressure and the mean molecular area on the subphase pH. The collapse pressure initially increases as the subphase pH is decreased and the monolayer becomes increasingly protonated. However, the collapse pressure becomes independent of subphase pH for values below approximately 4.0. The mean molecular areas, obtained by extrapolating the steepest part of the $\pi-A$ isotherm to $\pi = 0$, also depend on the subphase pH. As illustrated in Figure 3, for $5.0 \leq pH \leq 7.0$ the area occupied is 120 ± 1.2 $Å^2$ before increasing to approximately 128 ± 1.3 $Å^2$ when the pH is 4.0 or less. These results indicate that there is a limiting mean molecular area for both the fully deprotonated and protonated films. The data shown in Figure 3 correspond to a pK_a for the Qbpy ligand of the complex within the monolayer of approximately 4.3, which is indistinguishable from the pK_a found for the $Qbpy-QbpyH^+$ reaction when the complex is dissolved in aqueous/acetonitrile solution in the absence of perchlorate. Although the solubility of the complex depends on the identity of the counterion, the complex is typically sufficiently soluble in concentrated acid solutions to prevent the formation of stable monolayers. This behavior currently prevents us from investigating these monolayer films below approximately pH 3. However, the similarity of the pK_a

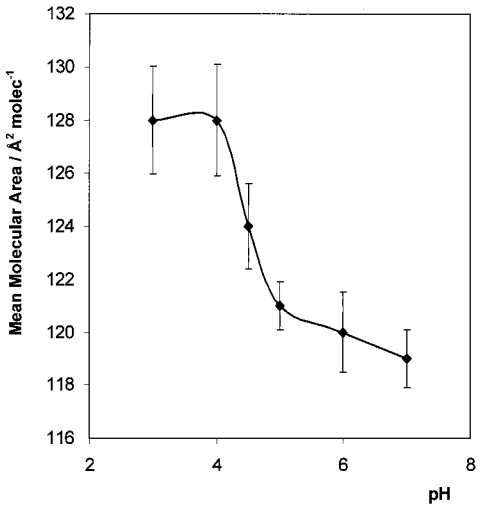

Figure 3. Effect of subphase pH on the mean molecular area within $[Os(dpp)_2Qbpy](ClO_4)_2$ monolayers.

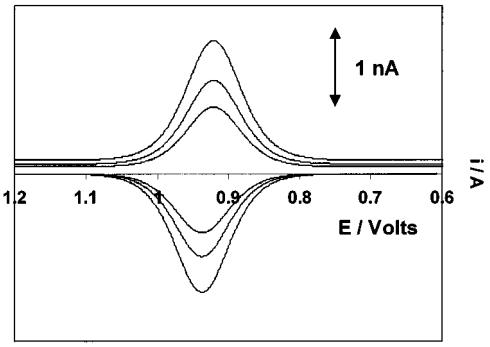

Figure 4. Horizontal touch voltammograms for a Langmuir monolayer of $[Os(dpp)_2Qbpy](ClO_4)_2$ at a surface pressure of 52 mN m^{-1} (corresponds to a surface concentration of 1.8×10^{-10} mol cm^{-2}). The working electrode is a 5 μm disk platinum microdisk. Scan rates (top to bottom) are 10 000, 7000, and 5000 mV/s. The subphase pH is 3.0. Anodic currents are down; cathodic currents are up.

values for the complex both in solution and as a Langmuir monolayer suggests that the pK_a of the Qbpy ligand is not significantly affected by the formation of a dense molecular assembly.

Horizontal Touch Voltammetry. Figure 4 illustrates the horizontal touch voltammetry response of the monolayer obtained at a surface pressure of 52 mN m^{-1}, corresponding to the mean molecular area of 95 Å^2 molec^{-1}, where the subphase is 0.1 M $NaClO_4$ adjusted to pH 3.0 by adding concentrated $HClO_4$. For scan rates between 5000 and 10 000 mV/s, ΔE_P is close to zero, Gaussian shaped peaks are observed, and the peak current varies linearly with the scan rate. The charge under the voltammetric peak recorded with a 5 μm Pt disk electrode yields a surface concentration of 1.8×10^{-10} mol cm^{-2}, which is in acceptable agreement with the value of 1.7×10^{-10} mol cm^{-2} predicted on the basis of 95 Å^2 molec^{-1} obtained from the $\pi-A$ isotherm. This short time scale behavior is consistent with that expected for an immobile, electrochemically reversible couple where heterogeneous electron transfer across the electrode/monolayer interface is rapid compared to the time scale of the experiment. Moreover, the response is similar to that observed for either spontaneously adsorbed monolayers formed using this complex or where the microelectrode is forced through the monolayer directly into the subphase. These observations suggest that at short times the observed current is dominated by the small fraction of the Langmuir monolayer that is located

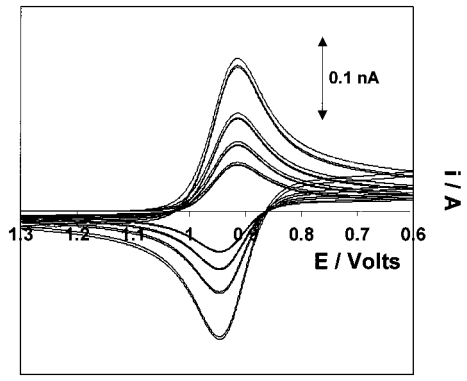

Figure 5. Horizontal touch voltammograms for a Langmuir monolayer at a surface pressure of 52 mN m^{-1} (corresponds to a surface concentration of 1.75×10^{-10} mol cm^{-2}). The working electrode is a 5 μm disk platinum microdisk. Scan rates (top to bottom) are 500, 200, 100, and 50 mV/s. The subphase pH is 3.0. Anodic currents are down; cathodic currents are up.

directly beneath the microelectrode and that its voltammetric response is nearly ideal.

As the experimental time scale is increased, one might expect that lateral electron transport occurring by either a electron self-exchange (hopping) mechanism or via lateral translational diffusion would allow redox centers located beyond the outer edge of the Pt disk to undergo redox reactions. Because lateral charge transport is typically a rather slow process,[25] the relative contribution from diffusion to the overall current will *increase* with *decreasing* scan rates. Figure 5 exhibits horizontal touch voltammograms obtained for a 5 μm radius microelectrode at scan rates (ν) of 50, 100, 200, and 500 mV/s. The shapes of these voltammetric responses are independent of the scan rate over this range, the peak-to-peak separation, ΔE_P, is 65 ± 4 mV, the ratio of anodic to cathodic peak currents is unity within experimental error, and the peak current increases as $\nu^{1/2}$. These results are consistent with those expected for an electrochemically reversible couple undergoing an electron-transfer reaction that is controlled by a semi-infinite diffusion process over this range of experimental time scales.[20] While the diffusion-controlled responses observed are reminiscent of those reported previously using line-electrodes,[5,25] it is important to consider differences between the two approaches. In contrast to the line electrode technique that probes diffusion processes at the air/water interface, because of the glass shroud that insulates the platinum microdisk, the HTV approach employed here probes lateral diffusion at the glass/water interface. The thickness of the insulator (typically 1.5 mm) is significantly larger than the expected thickness of the diffusion zone that is created during the voltammetric experiments (ca. 10 μm). While future reports will address this issue directly by comparing line electrode and HTV measurements, we believe that lateral physical diffusion in the HTV experiments is perhaps slower than what might be observed for the same monolayer at the air/water interface. However, when the monolayers are fully compressed, and thus when electron hopping is the sole mode of charge transport, it is likely that the HTV method provides equally reliable values of the apparent lateral diffusion constants (D_{app}).

Dependence of D_{app} on Monolayer Compression. As discussed previously,[5,8,25] D_{app} can be evaluated from the slope of a plot of i_P vs $\nu^{1/2}$ in accordance with eq 1

$$i_P = (2.69 \times 10^5) n^{3/2} \Gamma l D_{app}^{1/2} \nu^{1/2} \qquad (1)$$

where n is the number of electrons transferred and l is the length of the line electrode or the circumference of the microelectrode

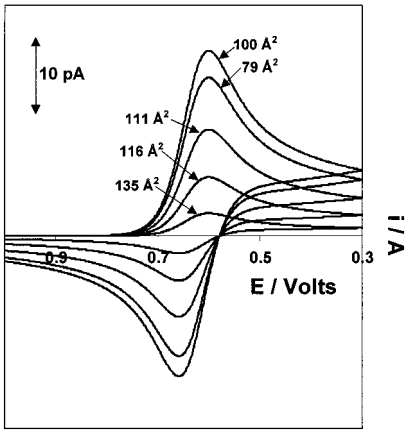

Figure 6. Dependence of the horizontal touch voltammetry recorded at 100 mV/s on the mean molecular area. The subphase is 0.1 M $NaClO_4$ adjusted to pH 3.0 by adding concentrated $HClO_4$. The working electrode is a 1 μm radius platinum microdisk.

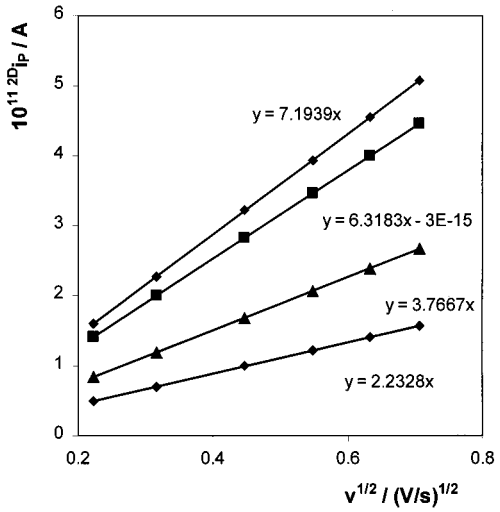

Figure 7. Plots of $i_{P,\,cathodic}$ vs the square root of the scan rate at molecular areas (top to bottom) of 100, 79, 111, and 116 Å^2. The subphase is 0.1 M $NaClO_4$, adjusted to pH 3.0 by adding concentrated $HClO_4$, and the working electrode is a 1 μm platinum microdisk.

in HTV experiments. Figure 6 shows the variation in the voltammetric response obtained at 100 mV/s as the mean molecular area is systematically varied from 135 to 79 Å^2 molec^{-1}, where the subphase contains 0.1 M $NaClO_4$ adjusted to pH 3.0 by adding concentrated $HClO_4$. The peak currents of these voltammograms clearly depend on the degree of monolayer compression with i_P initially increasing with increasing monolayer compression before decreasing when the mean molecular area decreases below approximately 100 Å^2 molec^{-1}. Figure 7 shows several examples of the corresponding i_P vs $\nu^{1/2}$ plots. In all cases these plots are linear for scan rates between 50 and 500 mV/s, suggesting that a semi-infinite linear diffusion process dominates the observed current and that eq 1 provides an appropriate description of the response. The slopes of these lines are proportional to the lateral electron transport rates, which can be expressed as D_{app}. In the range of surface concentrations explored in these slow scan rate experiments, the contribution from the monolayer located directly under the microelectrode is less than 25% of the total current, even at the highest scan rate of 500 mV/s used to investigate 2-D electron transport. Therefore, it appears that horizontal touch voltammetry provides an accurate measurement of the lateral charge transport diffusion coefficient, D_{app}, provided that slow scan rates are employed.

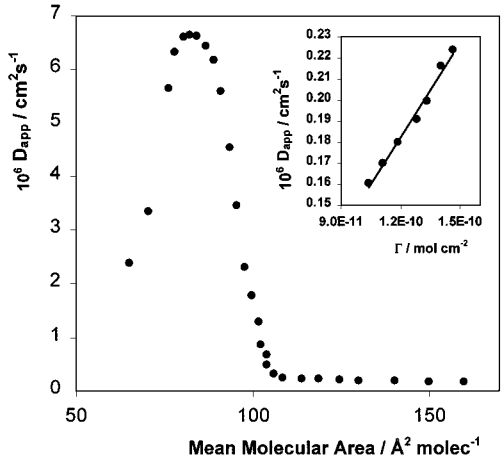

Figure 8. Plot of D_{app} obtained from horizontal touch voltammetry vs molecular area of $[Os(dpp)_2Qbpy](ClO_4)_2$. The subphase pH is 0.1 M $NaClO_4$, adjusted to pH 3.0 using concentrated perchloric acid.

Figure 8 illustrates the dependence of D_{app} on the mean molecular area. These data demonstrate that D_{app} increases from approximately 1.6×10^{-7} to 2.3×10^{-7} cm^2 s^{-1} as the mean molecular area decreases from 165 to 110 Å^2 molec^{-1}. However, further compression of the monolayer (particularly such that the mean molecular area decreases below 106 Å^2 molec^{-1}) causes a dramatic rise in the charge transport rate. This behavior is restricted to acidic pH conditions but is not sensitive to the perchlorate concentration in the subphase, suggesting that counterion diffusion does not limit the rate of charge transport through these monolayers.

When the monolayer exists in an expanded state (165−110 Å^2 molec^{-1}), physical diffusion of the Qbpy complexes as well as electron hopping may contribute to the observed diffusion coefficient. The theory of diffusive charge transport coupled to electron hopping has been extensively developed.[21−23] Under ideal conditions, where charge is transported entirely by physical diffusion, the apparent diffusion coefficient should be independent of the concentration of the redox active species. In contrast, if electron hopping plays a role in the charge transport mechanism, D_{app} will increase as the concentration of electroactive species is increased according to the following equation

$$D_{app} = D_{phys} + \frac{k_{ex}\delta^2 C}{6} \qquad (2)$$

where D_{phys} is the physical diffusion constant and the second term represents the diffusion constant due to electron hopping (D_e).[24] In eq 2, k_{ex} is the second-order electron self-exchange rate constant, δ represents the center-to-center distance of the two redox species as they exchange an electron, and C is their concentration. A 2-D version of the electron hopping diffusion constant, developed by Charych and co-workers,[7] features Γ, the surface concentration of redox species, and a two-dimensional version of a self-exchange rate constant, $^{2D}k_{ex}$ (cm^2 mol^{-1} s^{-1}):

$$D_e = \frac{^{2D}k_{ex}\delta^2\Gamma}{4} \qquad (3)$$

In view of the precursor complex model, $^{2D}k_{ex}$ was related to k_{ex} via

$$k_{ex} = {}^{2D}k_{ex}2\delta \qquad (4)$$

The inset of Figure 8 illustrates the dependence of D_{app} on the surface concentration of the $[Os(dpp)_2Qbpy](ClO_4)_2$ redox centers within the monolayer in the expanded region. These data reveal that D_{app} increases linearly from 1.6×10^{-7} to 2.3×10^{-7} cm^2 s^{-1} as the surface concentration is increased from approximately 1.0×10^{-10} to 1.5×10^{-10} mol cm^{-2}. It is important to note that our ability to accurately measure D_{app} for monolayers in which the mean molecular area is larger than about 160 Å^2 is limited by the low currents (picoamps) observed for the expanded monolayers when using microelectrodes with radii as small as 1 μm.

The linear dependence of D_{app} on the 2-D concentration shown in the inset of Figure 8 is consistent with the behavior predicted by the Dahms−Ruff[25] model described in eqs 2 and 3. Using eqs 2−4, the slope of the Figure 8 inset gives a self-exchange rate constant, k_{ex}, of approximately 1.0×10^8 M^{-1} s^{-1}. This value of k_{ex} is somewhat arbitrary since it is based on a value of 11.3 Å for δ, i.e., the minimum center-to-center distance obtained from the lowest mean molecular area of 110 Å^2 molec^{-1}. Since previous reports on liquid monolayer films of amphiphiles such as *N*-alkanecarboxamide ferrocenes show that the rate of physical diffusion decreases as the monolayer is compressed,[5,25] the slope of the inset of Figure 8 is likely to be reduced from its true value. Consequently, the value of k_{ex} obtained by analyzing the surface concentration dependence of D_{app} represents a lower limit. In conclusion, it appears that that both physical diffusion (which decreases with increasing monolayer compression) and electron self-exchange (which increases with increasing film compression and is the dominant effect) contribute to the overall charge transport rate in this range of monolayer compression.

The most striking feature of Figure 8 is that the apparent diffusion coefficient increases dramatically when the surface concentration of redox centers is increased above approximately 1.5×10^{-10} mol cm^{-2} (below ca. 110 Å^2 molec^{-1}). The maximum value of 6.6×10^{-6} cm^2 s^{-1} is reached at ca. 82 Å^2 molec^{-1}. We associate this behavior with the formation of a more compressed phase of $[Os(dpp)_2Qbpy](ClO_4)_2$, which, due to the smaller Os−Os distance, exhibits a higher redox conductivity. Under these conditions, classical percolation behavior is expected where the conductivity increases sharply as a result of increasing connectivity between domains of the conducting phase. Recent investigations of lateral electron hopping in the $Os(dpp)_3(ClO_4)_2$ system revealed a close correlation between theory and experiment, suggesting that for highly compressed monolayers the dominant mode of charge transport is percolation.[8] In the system considered here, fast electron hopping becomes the dominant charge transport mechanism only when there is significant interpenetration of the diphenylphenanthroline ligands following compression to MMA < 110 Å^2 molec^{-1}. In the absence of grazing incidence angle X-ray diffraction measurements that would provide direct information about the structure of this phase,[8] we have calculated an average Os−Os distance, r_{NN}, of 9.7 Å from the MMA, corresponding to the maximum value of D_{app} (82 Å^2 molec^{-1}; see Figure 8) on the assumption that the molecules are hexagonally close-packed. Provided that all redox centers within the assembly are electroactive, the unimolecular electron-transfer rate constant,[8] k_1, can be calculated as 2.8×10^9 s^{-1} using eq 5

$$D_{app,max} = \frac{1}{4} k_1 r_{NN}^{\ 2} \tag{5}$$

where $D_{app,max}$ is the maximum apparent diffusion coefficient observed ($6.6 \pm 0.2 \times 10^{-6}$ cm^2 s^{-1}). The corresponding bimolecular self-exchange rate constant, k_{ex}, can be calculated from the precursor complex model in which k_{ex} is expressed as the product of k_1 and K_P, a precursor complex "equilibrium constant"[5,26]

$$k_{ex} = k_1 K_p \qquad K_p = 4\pi N R^2 \delta R \tag{6}$$

where N is Avogadro's constant, R is the intermolecular distance separating the reactants in the transition state taken simply as δ, and δR (approximately 0.5 Å) is the "reaction zone thickness". The resulting k_{ex} is $1.0 \pm 0.05 \times 10^9$ M^{-1} s^{-1} for the $Os^{2+/3+}$ couple within the fully compressed Qbpy monolayer. This value is an order of magnitude greater than k_{ex} obtained above from the expanded region of the monolayer. While both of these values are subject to some approximations, to our best knowledge this is the first case in which compression of a Langmuir monolayer results in a significant increase of the rate of electron transfer. The increase could be due either to an increase of electronic coupling upon monolayer compression or to a decrease of the reorganization energy brought about by decreased hydration of the osmium centers in their more compressed state. These factors as well as the structure of the $[Os(dpp)_2Qbpy](ClO_4)_2$ monolayer will be considered in our later reports.

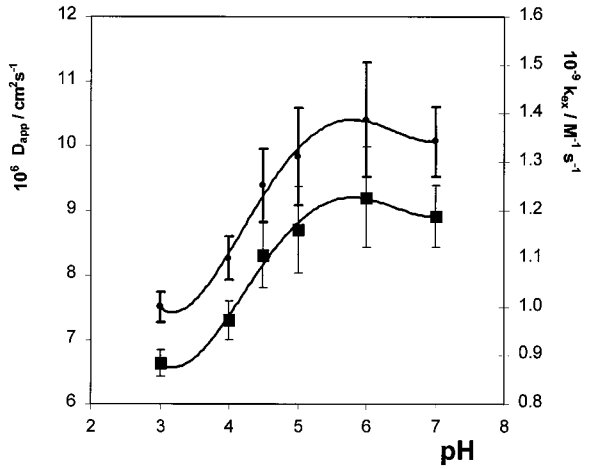

Figure 9. Dependence of the maximum D_{app} (solid squares, axis to the left) and self-exchange rate constants (solid circles, axis to the right) on the subphase pH.

Effect of Subphase pH on $D_{app,max}$. Because of its importance to a diverse range of areas including biological systems and chemical sensing, there is currently intense interest in the effect of protonation on electron-transfer reactions in both the ground[27,28] and excited states.[29] The Qbpy Langmuir monolayers considered here can provide an insight into how the rate of self-exchange depends on the extent of Qbpy protonation and hence the overall state of charge of the monolayer. The dependence of $D_{app,max}$ on the pH of the subphase is illustrated in Figure 9. The maximum diffusion coefficient in these monolayers depends on both the kinetics of electron hopping and the surface concentration of the redox sites. The mean molecular area at the maximum compression increases from 75 Å^2 at pH 7.0 to 82 Å^2 at pH 3.0 (see Figure 3). Therefore, given the smaller osmium−osmium distance found for the deprotonated monolayer, one would expect a higher D_{app} for the deprotonated than for the protonated monolayers. These data support our conclusion that electrostatic repulsion between protonated complexes causes their molecular areas to be larger for a given surface pressure. Figure 9 also shows the dependence of k_{ex} on subphase. Two limiting values of the self-exchange rate constant are

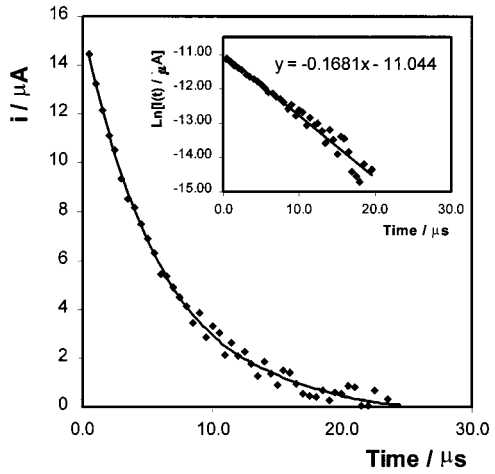

Figure 10. Current response for a 12.5 radius platinum microdisk in contact with a fully compressed $[Os(dpp)_2Qbpy](ClO_4)_2$ Langmuir monolayer. The overpotential, η, is 50 mV. The subphase is 0.1 M $NaClO_4$, adjusted to pH 3.0 using concentrated perchloric acid. The inset shows ln $i_F(t)$ vs t plots for the Faradaic reaction.

observed, with k_{ex} being $1.0 \pm 0.05 \times 10^9$ and $1.35 \pm 0.05 \times 10^9$ M^{-1} s^{-1} for fully protonated and deprotonated monolayers, respectively. Our current data do not allow us determine whether the decrease of k_{ex} caused by the protonation of the monolayer arises because of weaker coupling between the metal centers or because of an increase in the outer sphere reorganization energy of the system. However, previous studies on $[Os(dpp)_3]^{2+}$ monolayers[6,7] clearly demonstrate that changing the composition of the intervening medium by adding small volumes of an organic solvent to the subphase can dramatically affect the self-exchange rate constant.

Heterogeneous Kinetics. As illustrated in Figure 4, in on-trough voltammetric experiments it is possible to control the experimental time scale such that the current response is dominated by the redox centers located immediately under the microelectrode tip rather than by lateral charge transport. Similar behavior is observed if the microelectrode is forced through the monolayer into the subphase below. However, in horizontal touch experiments, if the experimental time scale is made sufficiently short, then not only is the contribution from lateral electron exchange negligible, but the rate of heterogeneous electron transfer across the electrode/monolayer interface will influence the voltammetric or amperometric response.

While there has been intense research into those factors that influence electron transfer across electrode/self-assembled monolayer interfaces,[30] relatively few systems exist that allow orientational effects on heterogeneous electron transfer to be probed. Previously, we have formed spontaneously adsorbed monolayers in which the quarterpyridyl ligand acts as a bridge between a $[Ru(bpy)_2]^{2+}$ redox center and the surface of a microelectrode.[14] In contrast, in the horizontal touch experiments on Langmuir films considered here, the quarterpyridyl ligand is in the aqueous subphase and electrical contact will occur through the diphenylphenanthroline ligands. Thus, by comparing the rates of electron transfer in spontaneously absorbed and Langmuir monolayers, it ought to be possible to gain some insight into orientational effects on electron transfer.

To address this issue, we have performed chronoamperometry on a microsecond time scale at microelectrodes in contact with Langmuir monolayers that are compressed to the point where the maximum D_{app} is observed. Figure 10 illustrates the current−time transient observed over a 25 μs time scale immediately after the potential was stepped from 0.60 to 0.95 V. This potential step triggers the Os^{2+} to Os^{3+} oxidation with a 50 mV overpotential ($\eta = E_{app} - E^{\circ\prime}$). For an ideal electrochemical reaction involving an immobile species, the Faradaic current following a potential step that changes the redox composition of the monolayer exhibits a single-exponential decay in time according to[31,32]

$$i_F(t) = kQ \exp(-kt) \tag{7}$$

where k is the apparent rate constant for the overall reaction and Q is the total charge passed in the redox transformation.

As discussed previously,[11,12,18,33] the microelectrodes used in measurements of this kind exhibit close to ideal responses in that both the ohmic loss and RC time constants for the electrodes are minimized by carefully selecting the electrode radius and by using a high concentration of supporting electrolyte. For example, for the experiment illustrated in Figure 10, the RC time constant is approximately 500 ns while the iR drop is less than 20 mV for times longer than approximately 5 μs. Therefore, it is possible to accurately measure the rate of heterogeneous electron transfer using this approach.

The linearity of the semilog plots shown in the inset of Figure 10 indicates that heterogeneous electron-transfer associated with oxidizing an $[Os(dpp)_2Qbpy](ClO_4)_2$ Langmuir monolayer is a first-order process. Since uncompensated resistance causes the applied potential, and hence the apparent rate, to evolve with time, nonlinear responses would be expected if substantial ohmic drop effects were present. Beyond the issue of iR drop, the linear responses illustrated in Figure 10 indicate that the local microenvironments, electron transfer distances, and degrees of electronic coupling between the redox centers and the electrode are similar for individual adsorbates within the monolayer. Given that the absolute value of the slope of the semilog plot represents the rate constant, it is apparent that heterogeneous electron transfer occurs very rapidly in this system. For example, even for a modest overpotential of 50 mV, the heterogeneous electron-transfer rate constant, k, for oxidation of the osmium centers is $1.7 \pm 0.2 \times 10^5$ s^{-1}.

We have investigated the rate of heterogeneous electron transfer for microelectrodes modified with spontaneously adsorbed monolayers[34] of $[Os(dpp)_2\ Qbpy]^{2+}$ and observed an electron-transfer rate of $1.2 \pm 0.3 \times 10^6$ s^{-1}, where the overpotential is 50 mV. We have also modeled the cyclic voltammetric responses of both Langmuir and spontaneously adsorbed monolayers using a nonadiabatic electron-transfer approach. This model indicates that the outer sphere reorganization energies, λ, of the two systems are similar. Therefore, it is unlikely that differences in λ cause the rate of heterogeneous electron transfer for the Langmuir monolayer to be approximately an order of magnitude smaller than that observed for the spontaneously adsorbed system where the Qbpy ligands contact the electrode. However, the experimental data are consistent with stronger electronic coupling existing between the $Os^{2+/3+}$ site and the electrode when the centers are chemisorbed on the Pt electrode. While our current data do not allow us to determine if this behavior arises because of differences in the electron-transfer distance, tunneling medium, or barrier, it is clear that the orientation of the complex, i.e., whether the Qbpy or dpp ligands contact the electrode, influences the electron-transfer rate.

It is of particular interest to compare homogeneous and heterogeneous rate constants for this system. Frequently, assuming that the free energy of activation for heterogeneous electron transfer, $\Delta G^{\ddagger}_{het}$, is only half that of the homogeneous reaction, $\Delta G^{\ddagger}_{homo}$, (because only one reactant has to be

reorganized) yields satisfactory agreement between the two preexponential factors.[35] However, taking $\Delta G^{\ddagger}_{het} = {}^1/_2\Delta G^{\ddagger}_{homo}$ and the transfer coefficient for heterogeneous electron transfer as 0.5 fails to yield satisfactory agreement between the two approaches with ratios of the preexponential being approximately 10^3 rather than unity under some experimental conditions.

Conclusions

A new Langmuir monolayer comprising of an osmium complex $[Os(dpp)_2\ Qbpy](ClO_4)_2$ with mixed hydrophobic/hydrophilic character has been produced. Unlike $[Os(dpp)_3](ClO_4)_2$ Langmuir monolayers, expanded liquid films exist in a range of low surface pressures that can be reversibly compressed and expanded. This result suggests that the unbound pyridine moieties of the Qbpy ligand interact strongly with the subphase at pH < 4.0. Both the mean molecular areas at all pressures and the collapse pressure depend strongly on the pH of the subphase, making this monolayer an attractive model system for investigating the distance dependence of lateral electron hopping.

By controlling the voltammetric time scale in horizontal touch voltammetric experiments, the rate of charge transport, D_{app}, through the Langmuir monolayers has been probed as the mean molecular area is systematically varied. Two distinct regions of surface pressures were observed in which the rates of electron self-exchange are substantially different. In the region of low pressures, where mean molecular areas (MMA) varied from 160 to 110 Å^2 molec^{-1}, a k_{ex} of 1.0×10^8 M^{-1} s^{-1} was obtained using a 2-D version of the Dahms−Ruff formalism. The creation of a more compressed phase of the osmium complexes at higher pressures (MMA < 110 Å^2 molec^{-1}, featuring Os−Os distance estimated at 9.7 Å) leads to an increase of the rate of electron self-exchange with a k_{ex} of 1.0×10^9 M^{-1} s^{-1} being obtained from the maximum value of D_{app}. An important advantage of the HTV technique developed here is its ability to measure the rate of the heterogeneous electron transfer. These measurements yield a rate constant smaller than that obtained for the same osmium complex chemisorbed on Pt via the pyridine groups of the Qbpy ligand. An important objective of future work is to resolve whether differences in the degree of electronic coupling or the free energy of activation for electron transfer are responsible for the differences in the observed rates of the homogeneous as well as heterogeneous electron transfer in these monolayer assemblies.

Acknowledgment. Financial support from Enterprise Ireland, the Irish Science and Technology Agency, under Strategic Research Grant ST/98/414, and International Collaboration Grant IC/1998/036 is gratefully acknowledged. The generous loan of hexachloroosmate and platinum microwires by Johnson Matthey under the loan scheme is deeply appreciated. M.M. acknowledges the support of the U.S. National Science Foundation under grant CHE-94226919.

References and Notes

(1) Andres, R. P.; Bielefiled, J. D.; Henderson, J. I.; Janes, D. B.; Kolgunta, V. R.; Kubiak, C. P.; Mahoney, W.; Osifchin, R. G. *Science* **1996**, *271*, 1705.
(2) Bardea, A.; Patolsky, F.; Dagan, A.; Willner, I. *Chem. Commun*. **1999**, *1*, 21.
(3) O'Regan, B.; Grätzel, M. *Nature* **1991**, *353*, 737.
(4) Pursch M.; Sander L. C.; Egelhaaf, H. J.; Raitza, M.; Wise, S. A.; Oelkrug D.; Albert, K. *J. Am. Chem. Soc*. **1999**, *121*, 3201.
(5) Charych, D. H.; Landau, E. M.; Majda, M. *J. Am. Chem. Soc.* **1991**, *113*, 3340.
(6) Charych, D. H.; Majda, M. *Thin Solid Films* **1992**, *210*, 348.
(7) Charych, D. H.; Anvar, D. J.; Majda, M. *Thin Solid Films* **1994**, *242*, 1.
(8) Lee, W.-Y.; Majda, M.; Brezesinski, G.; Wittek, M.; Möbius, D. *J. Phys. Chem. B.* In press.
(9) Acevedo, D.; Abrûna, H. D. *J. Phys. Chem*. **1991**, *95*, 9590.
(10) Acevedo, D.; Bretz, R. L.; Tirado, J. D.; Abrûna, H. D. *Langmuir* **1994**, *10*, 1300.
(11) Forster, R. J.; O'Kelly, J. P. *J. Phys. Chem*. **1996**, *100*, 3695.
(12) Forster, R. J. *Inorg. Chem*. **1996**, *35*, 3394.
(13) Forster, R. J.; Vos, J. G. and Keyes, T. E. *The Analyst* **1998**, *123*, 1905.
(14) Forster, R. J. and Keyes, T. E. *J. Phys. Chem. B.* **1998**; *102*, 10004.
(15) Sosnoff, C. S.; Sullivan, M.; Murray, R. W. *J. Phys. Chem. B.* **1994**, *98*, 13643.
(16) Fujihira, M.; Araki, T. *Chem. Lett*. **1986**, 921.
(17) Miller, C. J.; Bard, A. J. *Anal. Chem*. **1991**, *63*, 1707.
(18) Forster, R. J.; Faulkner, L. R. *J. Am. Chem. Soc*. **1994**, *116*, 5444.
(19) Zhang, X.; Bard, A. J. *J. Am. Chem. Soc.* **1989**, *111*, 8098.
(20) Bard, A. J.; Faulkner, L. R. *Electrochemical Methods: Fundamentals and Applications*, Wiley: New York, 1980.
(21) Blauch, D. N.; Savéant, J. M.; *J. Am. Chem. Soc*. **1992**, *114*, 3323.
(22) Fritsch-Faules, I.; Faulkner, L. R. *J. Electroanal. Chem*. **1989**, *263*, 237.
(23) Blauch, D. N.; Savéant, J. M. *J. Phys. Chem.* **1993**, *97*, 6444.
(24) Majda, M. Dynamics of Electron Transport in Polymeric Assemblies of Redox Centers. In *Molecular Design of Electrode Surfaces*; Murray, R. W., Ed.; Techniques in Chemistry Series; J. Wiley & Sons: New York, 1992; Chapter 4, p 159−206.
(25) Majda, M. Translational Diffusion and Electron Hopping in Monolayers at the Air/Water Interface. In *Organic Thin Films and Surfaces*; Ulman, A., Ed.; Academic Press: San Diego, 1995; Vol. 20, pp 331−347.
(26) Hupp, J. T.; Weaver, M. J. *J. Electroanal. Chem.* **1983**, *152*, 1.
(27) Baitalik. S.; Florke, U.; Nag K. *Inorg. Chem*. **1999**, *38*, 3296.
(28) O'Kelly, J. P.; Forster, R. J. *The Analyst* **1998**, *123*, 1987.
(29) Geisser, B.; Ponce, A.; Alsfasser, R. *Inorg. Chem*. **1999**, *38*, 2030.
(30) Forster, R. J. Ultrafast Electrochemical Techniques. In *Encyclopedia of Analytical Chemistry*; Wiley and Sons: New York, in press.
(31) Chidsey, C. E. D. *Science* **1991**, *251*, 919.
(32) Katz, E.; Willner, I. *Langmuir* **1997**, *13*, 3364.
(33) Forster, R. J., *Phys. Chem. Chem. Phys.* **1999**, *1*, 1543.
(34) Forster, R. J.; Keyes, T. E. Manuscript in preparation.
(35) Albery, W. J. *Electrode Kinetics*; Clarendon Press: Oxford, 1975.